Journal of Pharmaceutical and Biomedical Analysis 54 (2011) 324–330

Contents lists available at ScienceDirect

Journal of Pharmaceutical and Biomedical Analysis

journal homepage: www.elsevier.com/locate/jpba

Thermal decomposition of matrix metalloproteinase inhibitors: Evidence of solid state dimerization

Shelley R. Rabel Riley[a,g,*], Rodney D. Vickery[b,g], Gregory A. Nemeth[c,g], Michael J. Haas[d,g], Daniel J. Kasprzak[e], Michael B. Maurin[f,g]

[a] Northwest Missouri State University, Department of Chemistry/Physics, 800 University Drive, Maryville, MO 64468-6001, USA
[b] Bristol-Myers Squibb Company, Route 206 and Provinceline Road, Princeton, NJ 08540, USA
[c] Sanofi-Aventis, 1041 Route 202-206, Bridgewater, NJ 08807, USA
[d] Biocentury Publication, Inc., 223 Wilmington West Chester Pike, Chadds Ford, PA 19317, USA
[e] E.I. DuPont de Nemours and Company, Wilmington, DE 19880, USA
[f] Maurin Healthcare Consulting, P.O. Box 8217, Wilmington, DE 19803, USA
[g] Work performed at DuPont Pharmaceuticals Company, Wilmington, DE 19880, USA

ARTICLE INFO

Article history:
Received 28 June 2010
Received in revised form 29 August 2010
Accepted 7 September 2010
Available online 15 September 2010

Keywords:
Hydroxamic acid
Matrix metalloproteinase inhibitors
Thermal decomposition
Solid-state dimerization
Lossen Rearrangement

ABSTRACT

The thermal properties of three matrix metalloproteinase (MMP) inhibitors were investigated using a variety of instrumental methods. Differential scanning calorimetry revealed highly exothermic processes for all compounds above 200 °C, and thermogravimetric analysis resulted in significant step-wise weight losses at the temperatures corresponding to the exothermic transitions. Hot stage microscopy observations for several compounds showed evolution of gas bubbles from crystals at temperatures that correlated with the exotherms. Thermal decomposition involving the hydroxamic acid functional group was suspected and further evaluated using various analytical techniques including reversed-phase HPLC, LC–MS–MS, TGA-FTIR and NMR. The mechanism proposed in the thermal decomposition involves a Lossen Rearrangement to form a dimeric species containing a urea linkage.

1. Introduction

Matrix metalloproteinases (MMPs) are destructive collagenases that contain zinc at the active site. This class of collagenases is thought to be involved in cancer metastasis and the destruction of cartilage, leading to arthritis [1–3]. In addition, MMPs play a role in cardiovascular regulation (e.g. vessel tone, platelet aggregation). Inhibition of MMPs has been explored for indications such as atherosclerosis, aneurism, and reperfusion injury following heart transplants [4,5].

The hydroxamic acid functional group is a common structural feature found in molecules that inhibit MMPs. Hydroxamic acids are weak acids with typical pK_a values in the range 7–11, and studies have shown that ionization in aqueous solution occurs *via* dissociation of the O–H bond [6,7]. Two tautomers (keto- and iminol forms) of hydroxamic acids are known to exist. The keto-form is predominant in solution and serves as a site for metal chelation [8]. Therefore the presence of the hydroxamic acid plays an important role in binding zinc at the MMP active site, and is critical for activity of the compounds. The presence of the hydroxamic acid moiety is not limited to MMP inhibitors. The strong binding affinity of hydroxamic acids to metals has resulted in the inclusion of this group in compounds that inhibit other metalloproteinases. Suberoylanilide hydroxamic acid, a histone deacetylase inhibitor, was active in breast cancer cells [9], N-alkyl urea hydroxamic acids have been identified as peptide deformylase inhibitors with antibacterial activity [10], and macrocyclic hydroxamic acids have shown to be potent inhibitors of tumor necrosis factor α (TNF-α) converting enzyme with implications in autoimmune, infectious, and inflammatory responses [11].

In support of discovery efforts in identifying MMP inhibitors suitable for development of solid oral dosage forms, the physical chemical properties of three compounds (Fig. 1) were evaluated. Common features to all three compounds were the peptide-like backbone, and the presence of the hydroxamic acid functional group on each molecule. During the course of the physical chemical evaluation of the MMP inhibitors, it was noted that all compounds demonstrated atypical thermal behavior by differential scanning calorimetry (DSC). Consequently, further studies were initiated to better understand the nature of the thermal events using a combination of analytical techniques such as modulated DSC, reversed-phase HPLC, NMR, TGA-FTIR, and LC–MS–MS.

* Corresponding author. Present address: Northwest Missouri State University, Department of Chemistry/Physics, 2643 Garrett-Strong, 800 University Drive, Maryville, MO 64468-6001, USA. Tel.: +1 660 562 1605; fax: +1 660 562 1188.
E-mail address: sriley@nwmissouri.edu (S.R. Rabel Riley).

0731-7085/$ – see front matter © 2010 Elsevier B.V. All rights reserved.
doi:10.1016/j.jpba.2010.09.005

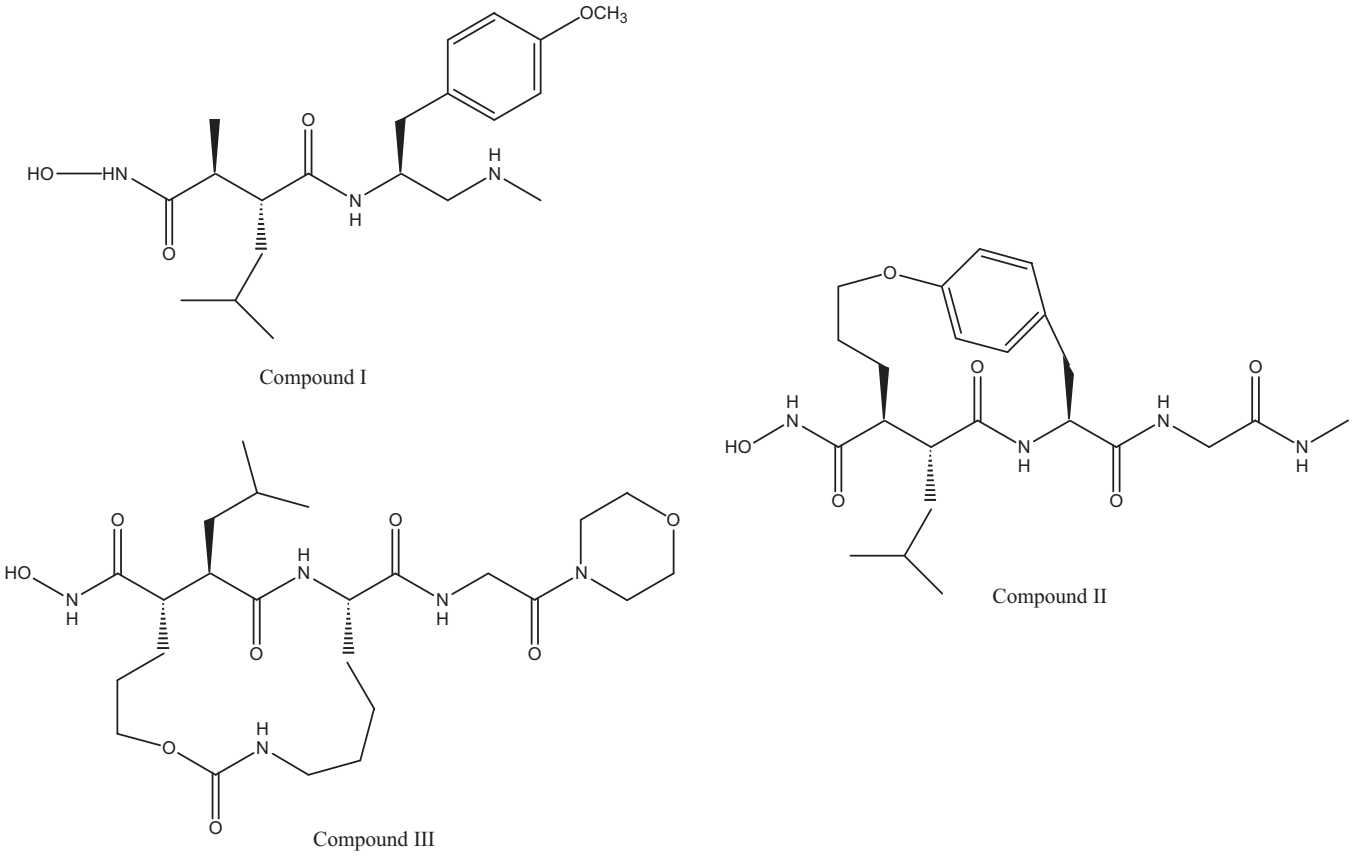

Fig. 1. Chemical structures of three MMP inhibitors.

2. Materials and methods

2.1. Materials

Compounds were prepared by Chemical and Physical Sciences (DuPont Pharmaceuticals Company), and were used as received. All other reagents were of analytical grade or higher. House deionized water was passed through a Milli-Q® ion exchange cartridge system resulting in a specific resistance of greater than 18 MΩ-cm.

2.2. Thermal analysis

The thermal properties of compounds were characterized with hot stage microscopy (Mettler Hot Stage FP82 and Central Processor FP80), and a Leitz Orthoplan-pol polarizing microscope. Samples were suspended in high viscosity microscope immersion oil (1250 CS) to allow visualization of gas evolution from crystals during hot stage microscopy experiments. Differential Scanning Calorimetry (DSC 910, TA Instruments) with a heating rate of 10 °C/min, and thermogravimetric analysis (TGA) with a heating rate of 10 °C/min (Hi-Res TGA 2950, TA Instruments) were utilized with data analysis *via* a thermal analyzer (Analyzer 2100, TA Instruments). In DSC analysis, the DSC cell was purged with nitrogen at 50 cc/min. Nitrogen flow rates of 40 and 60 cc/min were employed for the TGA balance and furnace, respectively.

2.3. LC–mass spectrometry

LC–MS–MS experiments were performed on a Finnigan TSQ7000 triple-quadrupole mass spectrometer operating in positive-ion electrospray ionization (ES+) mode and coupled to a Hewlett-Packard HP 1100 HPLC system. Liquid chromatography was performed on a C-18 column (150 mm × 4.6 mm, 5 μm) at a flow rate of 1.0 mL/min. The separation was performed under gradient conditions with a linear ramp from 0 to 100% Mobile Phase B over 10 min followed by an isocratic segment from 10 to 12 min. Mobile Phase A consisted of acetonitrile:water:acetic acid (10:90:0.05, v/v/v) and Mobile Phase B consisted of acetonitrile:water:acetic acid (95:5:0.05, v/v/v). Mobile phase B was maintained for the 2 min isocratic segment following the gradient. LC–MS experiments utilized a scan range of 150–1000 Da at 1 scan/s in ES+ mode, while LC–MS–MS experiments used the same HPLC conditions and MS–MS was performed by selecting the ion of interest (m/z 863) in the first quadrupole, subjecting it to 60-eV collisions with 1.0 Torr argon gas in the second quadrapole and detecting fragments in the third quadrapole using a scan range of 80–880 Da at 1 scan/s.

The exact mass analysis of Compound II degradant was performed on a Finnigan MAT95S reverse-geometry sector mass spectrometer equipped with an electrospray ionization sprayer interface and operating under high-resolution ES+ conditions (R = 6000). Sample was introduced into the system *via* flow-injection. Exact mass measurements were made by bracketing the ion of interest (m/z 863) with two reference ions of known exact mass from polypropylene glycol, and then interpolating. Four replicate measurements were made and the average value for the measured exact mass taken. Within the typical limits of error for this instrument and this type of experiment (±3.0 mDa), only one likely formula was determined.

2.4. NMR

The NMR data were acquired on a Varian Inova 600 MHz NMR. Samples were used as received and dissolved in dimethylsulfoxide-d_6 (DMSO-d_6). The NMR data was referenced to the solvent signals

at 2.49 ppm for proton and 39.5 ppm for carbon-13. All spectra were obtained at 30 °C. All data were acquired using an inverse detection probe with a *Z*-axis field gradient. Samples were analyzed using NMR, gradient enhanced proton shift correlated NMR (gCOSY), gradient enhanced proton-carbon shift correlated NMR (gHSQC) and long range gradient enhanced proton-carbon shift correlated NMR (gHMBC). The ^{1}H spectrum was recorded with a digital resolution of 0.25 Hz/pt (AT = 4.06 s), a tip angle of 30° and a relaxation delay of 2.0 s. ^{1}H–^{13}C gradient enhanced correlation spectra were obtained using a value of 140 Hz for $^{1}J_{C-H}$ and 7 Hz for $^{3}J_{C-H}$.

2.5. TGA-FTIR

A weighed portion of Compound III was positioned in the heating zone of the TGA apparatus (TA Instruments, Model 950 TGA) inside a quartz tube. The tube was sealed under a nitrogen purge gas at a constant flow rate (80 cc/min). The sample was heated to 300 °C at a programmed rate of 5 °C/min. The evolved gases were swept through a 20 cm IR gas cell that was scanned continuously by the FTIR spectrometer (Nicolet 20SX FTIR). The cell was maintained at a temperature of 250 °C to avoid condensation of higher boiling components. Infrared spectra of gaseous components were used to identify evolved gases and, combined with thermal data from the TGA, to determine evolution temperatures. TGA-FTIR experiments on Compound II were performed on a TGA apparatus (TA Instruments, Model 2950) equipped with a NEXUS 670 FTIR (Nicolet). Prior to initiation of the TGA-FTIR analysis of Compound II, the TGA system was purged with nitrogen (90–110 cc/min) while employing a heating program with a rate of 10 °C/min up to 100 °C and a subsequent isothermal segment at 100 °C for 5.0 min. Following this system purge, the sample was positioned in a nitrogen stream (90–110 cc/min) and subjected to a heating rate of 2.5 °C/min from 25 °C to 250 °C. Gases were detected in a similar fashion to Compound III and the data analysis was accomplished using Omnic, Search, Report, and Series Software (versions 5.1a or 5.1b).

2.6. Chromatography

A gradient reversed-phase HPLC method was used to analyze the post-TGA recovered samples. Analysis was performed using a Waters Symmetry C_{18} column (4.6 mm × 250 mm) at a temperature of 30 °C and a flow rate of 1.0 mL/min with UV detection at 230 nm. The gradient program was linear over 14 min with an initial mobile phase of acetonitrile:water:trifluoroacetic acid (10:90:0.05, v/v/v) and a final mobile phase consisting of acetonitrile:water:trifluoroacetic acid (30:70:0.05, v/v/v).

3. Results

3.1. DSC/TGA/hot stage microscopy

The overlays of the DSC and TGA thermograms for Compounds I, II and III are shown in Figs. 2–4. The DSC thermograms for all three compounds showed high energy exothermic transitions above 200 °C followed by endotherms. In all cases, a significant step weight loss accompanied the exothermic events with weight losses of 17.5%, 6.8% and 5.9% for Compounds I, II and III, respectively. The initial exotherm for Compound II was shown to be non-reversible when analyzed by modulated DSC [12]. Observations from hot stage microscopy for Compound II included a violent evolution of gas from the crystals at 211 °C. Similar observations were made for Compound III, which demonstrated bubbling at 253 °C. In both cases the evolution of gas correlated with the temperature of the exothermic transitions in DSC analysis. While no obvious release of gas was observed by hot stage microscopy for Compound I, the material appeared to darken at 150 °C, followed by partial melting at 230 °C with possible recrystallization. The thermal behavior of Compound I appears more complex, which may explain the multiple exothermic/endothermic events in the DSC thermogram. Results from DSC, TGA and hot stage microscopy of all three compounds were suggestive of thermal decomposition and additional studies were initiated to further characterize the nature of the exothermic transitions.

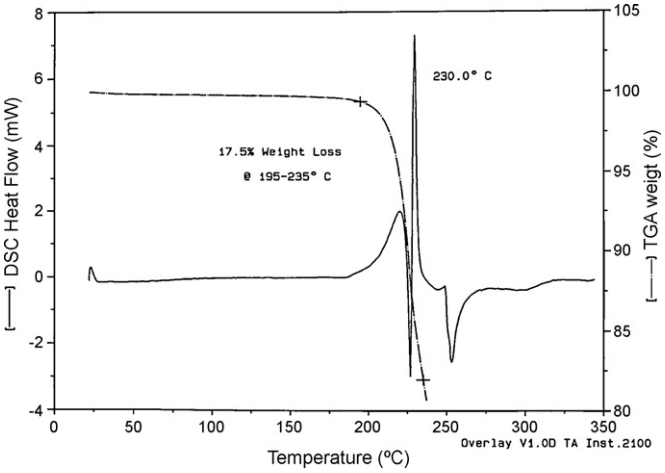

Fig. 2. Overlay of DSC/TGA thermograms for Compound I.

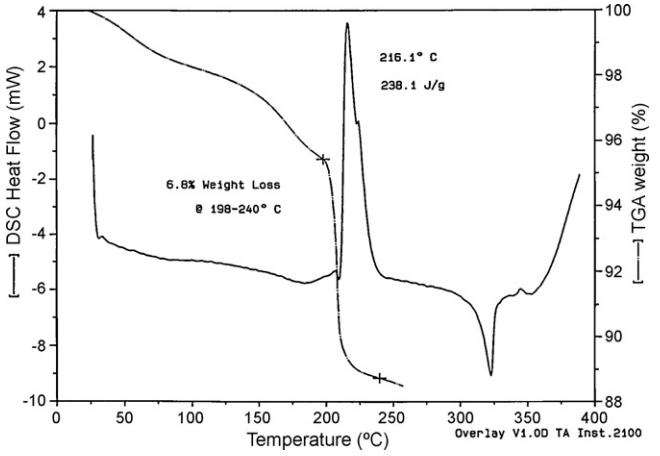

Fig. 3. Overlay of DSC/TGA thermograms for Compound II.

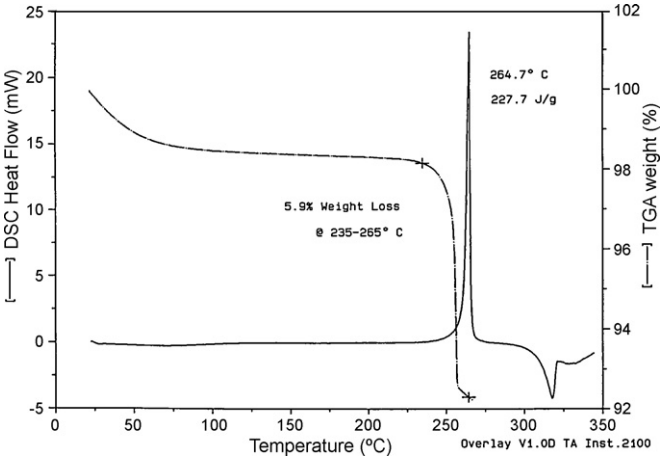

Fig. 4. Overlay of DSC/TGA thermograms for Compound III.

3.2. HPLC analysis

Compound II was heated to 260 °C, the material was recovered and analyzed by reversed-phase HPLC. The chromatograms of Compound II as received and post-heating are shown in Fig. 5. The parent peak initially present at 11.4 min was not observed in the post-heating sample, but rather the appearance of a more lipophilic compound accounting for approximately 80% of the material and eluting at approximately 20 min was observed along with minor degradants.

Similarly, Compounds I and III were heated through the exothermic transitions and analyzed by HPLC. HPLC results for Compound III showed no parent remaining and one major degradant at a relative retention time of 1.2. There was no parent remaining for Compound I and there were five main degradant peaks in the chromatogram with a multitude of smaller peaks detected.

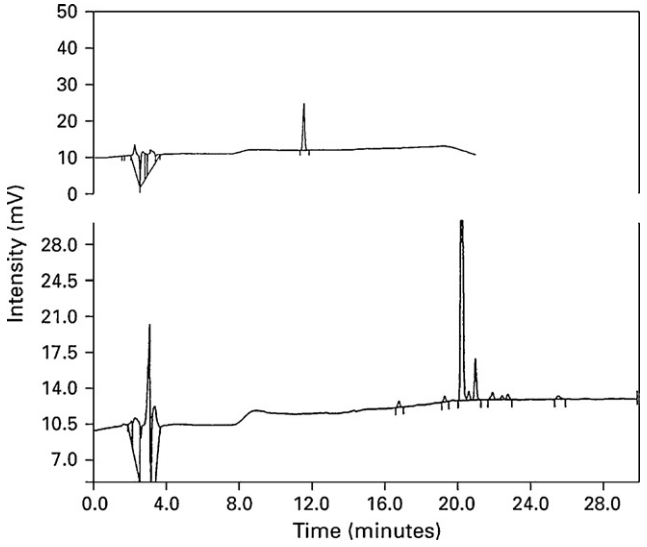

Fig. 5. Chromatograms of Compound II showing the material "As Received" (top) and "Recovered" material after heating through the exothermic transition to 260 °C (bottom).

3.3. Mass spectrometry and NMR analysis

LC–MS and LC–MS–MS results on the post-TGA sample of Compound II are shown in Fig. 6. The major degradant resulted in an $(M+H^+)$ ion of 863.4 compared to the staring material mass of 462.6. Exact mass measurements on the m/z 863 ion resulted in an exact mass of 863.5020 (±0.0007) Da from an average of four measurements, giving a molecular formula of $C_{45}H_{66}N_8O_9$. LC–MS–MS analysis on the m/z 863 ion gave major fragment ions of 419, 331, 321, 303, 205, and 188. There were no major fragments above m/z

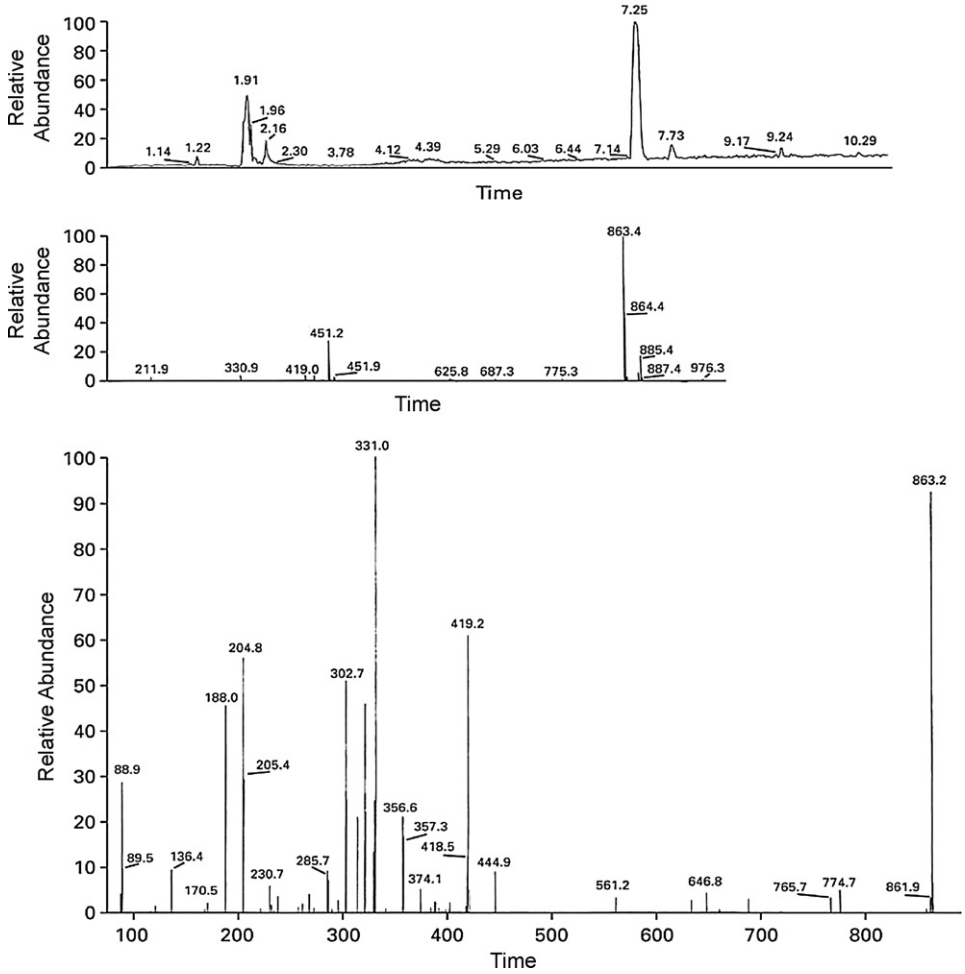

Fig. 6. LC–MS analysis of Compound II after heating material to 260 °C. The spectrum of the main degradant shows a $(M+H^+)$ ion of 863. The early eluting peaks appear to be predominantly solvent clusters. The LC–MS–MS spectrum of the parent ion shows fragments of 419, 331, 321, 303, 205 and 188 with no major fragments above m/z 419, with the exception of a weak signal at m/z 445.

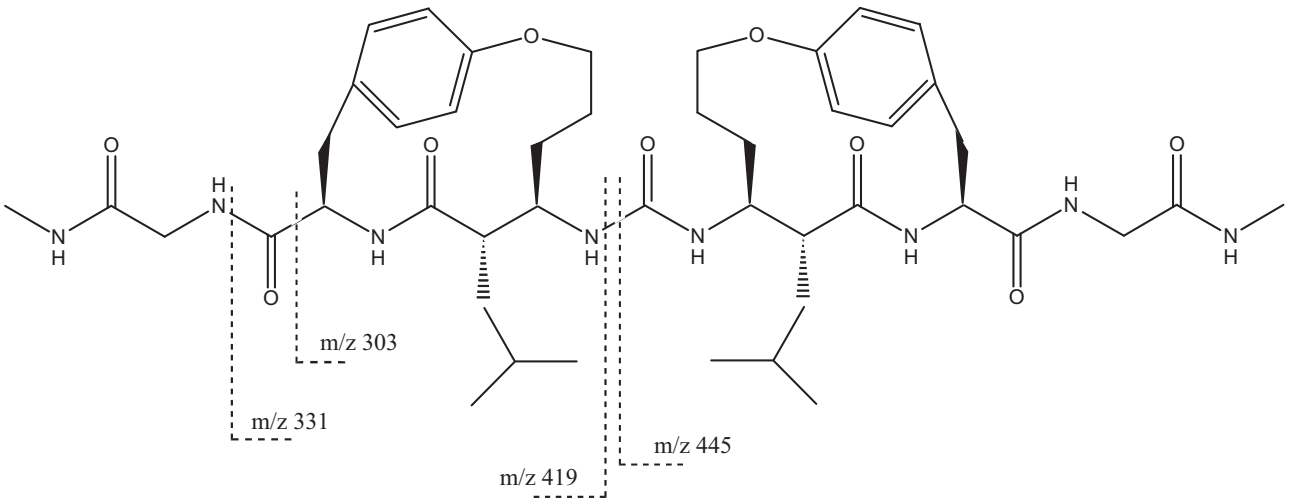

Fig. 7. Proposed dimeric degradant formed through thermal decomposition of Compound II.

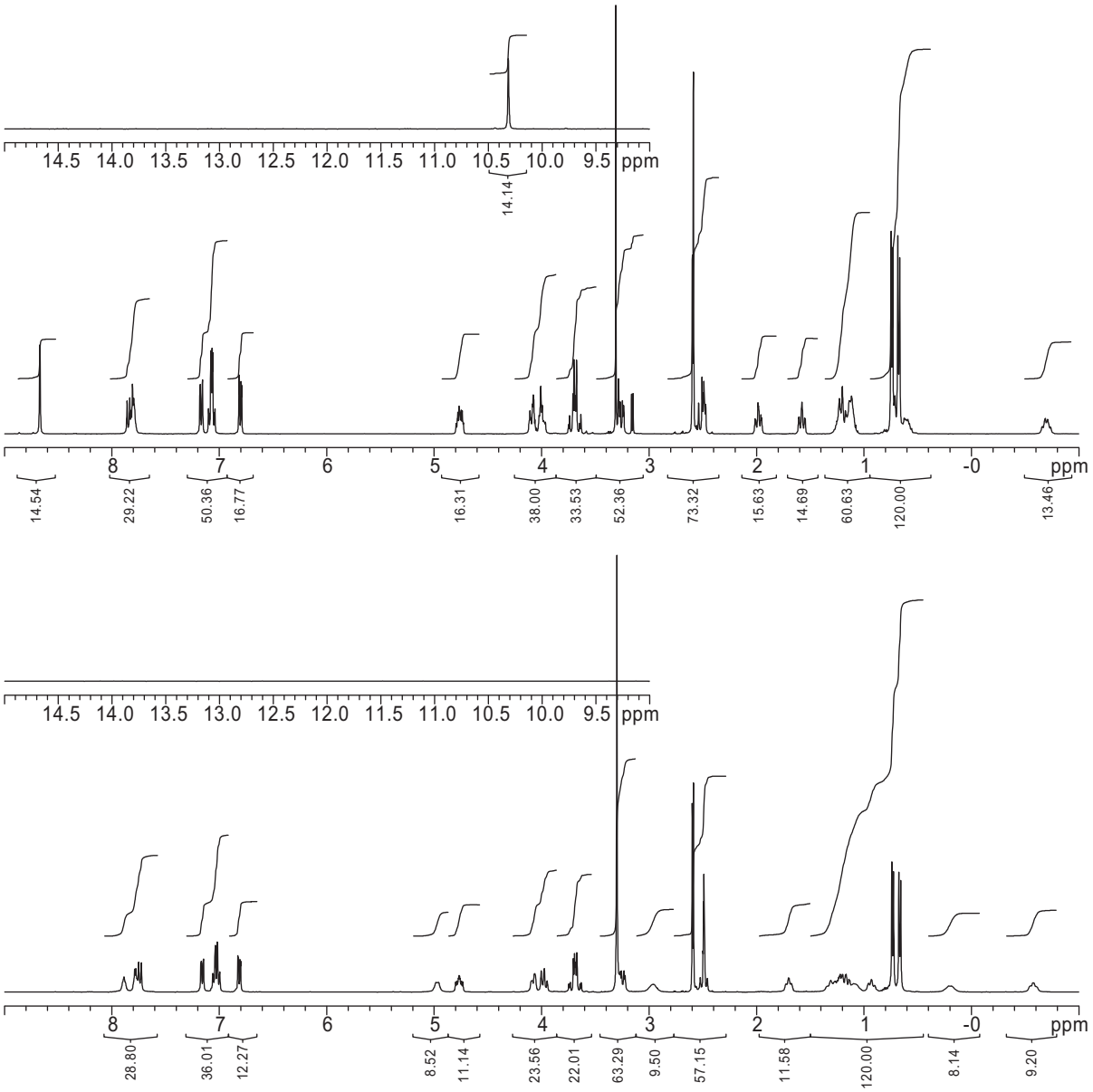

Fig. 8. NMR spectra of Compound II "As Received" (top), and after heating Compound II to 260 °C (bottom).

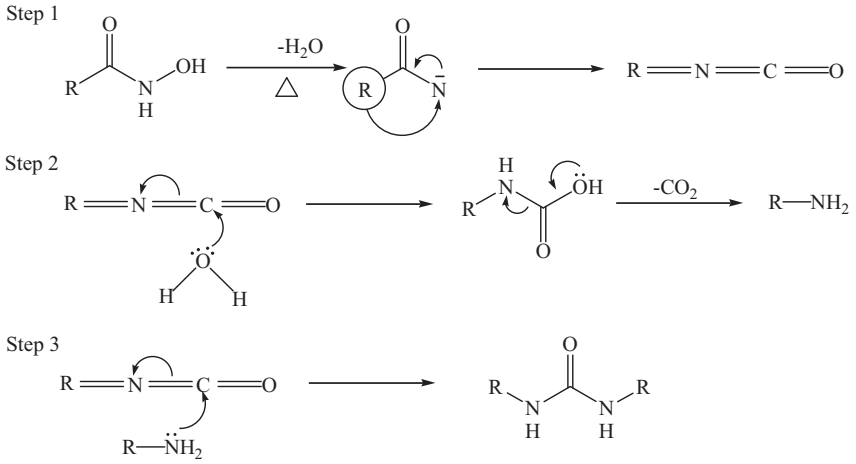

Fig. 9. Schematic of Lossen Rearrangement mechanism, and subsequent steps to form the dimeric species of Compound II.

419, with the exception of a weak signal at *m*/*z* 445. Therefore LC–MS–MS data indicated the presence of a dimeric compound (Fig. 7) that has two halves with molecular weights of 418 and 444. Compound II was also analyzed by NMR before and after heating (Fig. 8) and the results were consistent with the proposed dimeric structure. With the exception of two downfield resonances at 10.3 and 8.7 ppm that were initially present in the ^{1}H NMR spectra and assigned to the protons on the hydroxamic acid, the degradant shows all the same resonances observed in the pre-heated material. A new resonance was observed at 5 ppm and this signal has been assigned to the protons on the urea linkage of the degradant. In addition, the proton on the carbon adjacent to the nitrogen of the urea has shifted downfield 1 ppm and is coupled with the proton on the urea nitrogen.

3.4. TGA-FTIR analysis

Sufficient quantities of only Compounds II and III were available for analysis by TGA-FTIR. Analysis of Compound III resulted initially in the release of methanol, which was likely residual solvent from the drug substance isolation process, in the temperature range from ambient to 150 °C. A major gas evolution peak occurred at approximately 260 °C, which corresponded to the exotherm in the DSC thermogram. Gases detected during this transition included carbon dioxide, ammonia, water, and unidentified aliphatic material. These gases, except for water, continued to evolve slowly until the end of the analysis. TGA-FTIR analysis results of Compound II showed the predominant gases evolved were carbon dioxide and water, and the temperature at which these gases were released also correlated with the weight loss by TGA and the DSC exotherm for this compound.

4. Discussion

Given that the hydroxamic acid functional group was common to all three MMP inhibitors and the thermal behavior was similar for each compound tested, it was surmised that this was likely the site at which thermal degradation was occurring. Initially, the loss of the hydroxylamine was proposed since this loss was consistent with the TGA losses for Compounds II and III, in which theoretical weight losses of hydroxylamine would be 6.7% and 5.9%, respectively, as compared to the observed weight losses of 6.8% and 5.9%.

Initial mass spectrometry results for Compound II (post-heating) did not detect the presence of the dimer, presumably due to the instability of that species during analysis. These early results seemed to point to the loss of hydroxylamine leaving an aldehyde group on the degradant. However, NMR data was not consistent with the presence of an aldehyde. Although the signals from the protons on the hydroxamic acid (10.3 and 8.7 ppm) were no longer present in the NMR spectra of the heated material, there was no evidence of an aldehyde or a carboxylic acid, which could have resulted from hydrolysis of the aldehyde.

Subsequent LC–MS analysis of the heated material from Compound II did detect a high molecular weight dimer compound, and based on this data and the NMR data, the structure in Fig. 7 was proposed. The degradation product from thermal decomposition of compound II is likely formed *via* a Lossen Rearrangement (Fig. 9) in which a reactive isocyanate intermediate is formed. The isocyanate

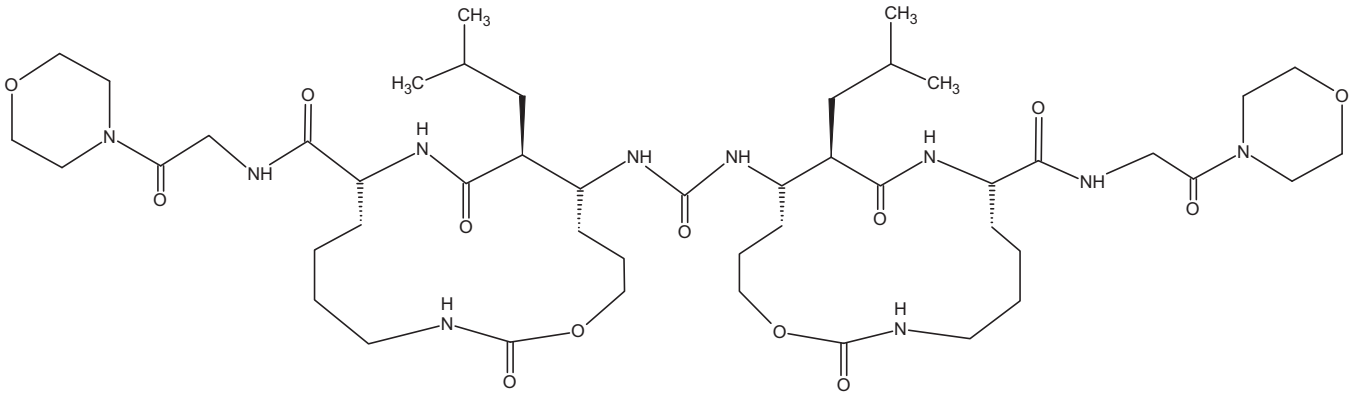

Fig. 10. Proposed structure of the dimer resulting from Lossen Rearrangement of Compound III.

intermediate can be hydrolyzed to form a primary amine [13]. The amine can then attack any remaining isocyanate species resulting in a urea linkage and dimer formation.

The TGA-FTIR results for both Compounds II and III, in which the predominant gases detected, were water and carbon dioxide, would also be consistent with this mechanism. In addition, the weight losses in TGA would be reasonable since for every dimer formed, carbon dioxide and water totaling 62 mass units would be lost, and result in weight losses of 6.7% and 5.9%, respectively.

Thermogravimetric analysis of Compound I resulted in a much larger than expected weight loss of 17.5%, as compared to a theoretical value of 7.9% for a mechanism similar to the other two compounds. Given the complexity of the DSC analysis for Compound I, it is likely that additional events (i.e. decomposition by multiple routes or solvent loss) may account for the additional weight loss for that particular compound, and would be consistent with HPLC results in which multiple degradants were observed for the post-TGA material.

5. Conclusions

Atypical thermal properties have been observed for MMP inhibitors in these and other laboratories [14]. Other groups have attributed the thermal events to either recrystallization or decomposition, however a degradation route was not previously proposed. The common structural feature for all compounds was the presence of the hydroxamic acid functional group. Based on traditional DSC and TGA results, thermal degradation of the hydroxamic acid was suspected and further characterized. Supplemental data from TGA-FTIR, LC–MS–MS and NMR suggested the formation of a dimeric species through a Lossen Rearrangement in the case of Comopund II. This type of rearrangement reaction has been reported for hydroxamic acids in solution [15,16]; however to our knowledge the Lossen Rearrangement in the solid state has not been previously described. Based on TGA-FTIR data for Compound III and the propensity for hydroxamic acids to degrade via the Lossen Rearrangement, it likely undergoes the same type of degradation to form the urea linked dimeric species proposed in Fig. 10. Multiple competing paths for degradation of Compound I would appear to exist to give various by-products, which were not identified. The thermal degradation of the three MMP inhibitors in this study occurred at temperatures above 200 °C, and therefore would not be considered to be problematic under normal processing/storage conditions encountered in solid dosage form development. However, given the presence of the hydroxamic acid group across a wide range of metalloproteinase inhibitors along with molecular structural variations surrounding this functional group, the possibility of degradation *via* the Lossen Rearrangement could potentially impact compound stability at lower temperatures than those observed in these studies. The application of multiple analytical techniques in the characterization of solid state degradation presented herein was effective in elucidating the structure of the dimeric species formed, and the mechanism by which hydroxamic degradation occurred.

Acknowledgements

The authors wish to acknowledge Kiho Lee and Carl Decicco for their input regarding rearrangement mechanisms, and Stephen Anderson for assistance in the TGA-FTIR analysis of Compound II.

References

[1] D.A. Fishman, Y. Liu, S.M. Ellerbroeck, M.S. Stack, Lysophatidic acid promotes matrix metalloproteinase (MMP) activators and MMP-dependent invasion in ovarian cancer cells, Cancer Res. 61 (2001) 3194–3199.
[2] M. Brennan, Drug development: two approaches combined to design novel class of collagenase inhibitors, Chem Eng. News (1996 Oct. 28) 9–10.
[3] R.J. Cherney, C.P. Decicco, D.J. Nelson, et al., Potent carboxylate inhibitors of stromelysin containing P2′ piperazic acids and P1′ biaryl moeities, Bioorg. Med. Chem. Lett. 7 (1997) 1757–1762.
[4] G. Dormán, K. Kocsis-Szommer, C. Spadoni, P. Ferdinandy, MMP inhibitors in cardiac diseases: an update, Rec. Pat. Cardiovasc. Drug Discov. 2 (2007) 1–9.
[5] V. Falk, P.M. Soccal, J. Grönenfelder, G. Hoyt, T. Walther, R.C. Robbins, Regulation of matrix metalloproteinases and effect of MMP-inhibition in heart transplant related reperfusion injury, Eur. J. Cardiothorac. Surg. 22 (2002) 53–58.
[6] B. Chatterjee, Donor properties of hydroxamic acids, Coord. Chem. Rev. 26 (1978) 281–303.
[7] R. Senthilnithy, S. Weeraginghe, D.P. Dissanayake, Stability of hydroxamate ions in aqueous medium, J. Mol. Struct. Theochem. 851 (2008) 109–114.
[8] B.A. Holmn, M. Isabel Tejedor-Tejedor, W.H. Casey, Hydroxamate complexes in solution and at the goethite–water interface: a cylindrical internal reflection fourier transform infrared spectroscopy study, Langmuir 21 (1997) 2197–2206.
[9] P. Bali, et al., Activity of suberoylanilide hydroxamic acid against human breast cancer cells with amplification of Her-2, Clin. Cancer Res. 11 (2005) 6382–6389.
[10] C.J. Hackbarth, et al., N-alkyl urea hydroxamic acids as a new class of peptide deformylase inhibitors with antibacterial activity, Antimicrob. Agents Chemother. 46 (2002) 2752–2764.
[11] C.B. Xue, et al., Discovery of macrocyclic hydroxamic acids containing biphenylmethyl derivatives at P1′, a series of selective TNF-α converting enzyme inhibitors with potent cellular activity in the inhibition of TNF-α release, J. Med. Chem. 44 (2001) 3351–3354.
[12] S.R. Rabel, J.A. Jona, M.B. Maurin, Applications of modulated differential scanning calorimetry in preformulation studies, J. Pharm. Biomed. Anal. 21 (1999) 339–345.
[13] M.B. Smith, J. March (Eds.), March's Advanced Organic Chemistry: Reactions Mechanisms and Structure, 5th ed., John Wiley & Sons, New York, 2001, p. 985.
[14] A.R. Nanda, S. Roy, P. Tyle, Preformulation study of a novel matrix metalloproteinase (MMP) inhibitor, AG3340, and its salts, for use in anticancer drugs, in: AAPS Annual Meeting and Exposition, Boston, MA, November 2–6, 1997.
[15] C.D. Hurd, L. Bauer, A novel rearrangement of hydroxamic acids using sulfonyl chlorides, J. Am. Chem. Soc. 76 (1954) 2791–2792.
[16] B. Hirrlinger, A. Stolz, Formation of a chiral hydroxamic acid with an amidase from rhodococcus erythropolis MP50 and subsequent chemical Lossen Rearrangement to a chiral amine, Appl. Environ. Microbiol. 63 (1997) 3390–3393.